# Influence of MeV helium implantation on deuterium retention in radiation damaged tungsten

E. Markina, M. Mayer*, S. Elgeti (Lindig) and T. Schwarz-Selinger

*Max-Planck-Institut für Plasmaphysik, EURATOM Association, 85748 Garching, Germany*

## Abstract

The influence of helium implanted with MeV energy on deuterium retention in damaged tungsten was investigated. Damage was introduced into the material using self-ion implantation. Two different cases – low (0.02 dpa) and high (0.89 dpa) W damage levels were investigated. Helium was introduced into the resulting damage zone using MeV ion implantation. Different He fluences were applied to investigate the He concentration dependency between 0 and 1000 ppm. D and He retention was investigated by ion beam analysis and thermal desorption spectroscopy. No helium desorption under thermal treatment up to 2000 K was observed. In both high and low damage level cases He does not affect the maximum D concentration within the damaged zone. For the 0.89 dpa and high He fluence samples a significant enhancement of D concentration behind the damaged zone was observed. In the lower damage case D transport within the damaged zone and further into the bulk was slowed down significantly even by lower He concentrations.

*Corresponding author: tel.: +49 89 3299 1639, e-mail: matej.mayer@ipp.mpg.de (Matej Mayer)

## 1. Introduction

In future fusion devices tritium will be used as a fuel element for the fusion reaction. Its radioactivity rises a safety concern for the fusion reactor design in terms of the retention properties of the plasma facing materials. The first wall and divertor parts of a future fusion reactor will be subjected to high fluxes of charged particles, neutral atoms, and neutrons [1]. All these processes can affect hydrogen retention in PFMCs.

For future fusion power reactors like DEMO tungsten has been suggested as a candidate for the divertor materials also due to its favorable hydrogen retention properties.

One of the above mentioned charged particles species are the alpha particles originating from the fusion plasma. This aspect of helium influence on hydrogen retention in tungsten has already been widely investigated for example by Alimov [2] and Ueda [3]. Both authors used He implantation from a plasma discharge i.e. low energetic He implantation. They observed a strong suppression of the diffusion of deuterium into tungsten, with a decrease of the deuterium concentration in depths of 1-7 μm by about one order of magnitude. Blistering of tungsten was also strongly suppressed by the addition of helium. These findings were explained by the formation of helium bubbles in the near-surface layer, which act as diffusion barrier for D. Other groups like Haasz and Lee [4] used ion beam implantation with He ion energies in the keV range. Lee assumed the formation of a helium-vacancy complex $He_nV_m$ at his exposure conditions [4] and similar to the plasma exposure studies found a suppression of D transport by He.

The other factor which can affect hydrogen retention in plasma facing materials in a fusion reactor are high energetic neutrons originating also from the fusion reaction. Fast fusion neutrons result in displacement damage and transmutation of tungsten to rhenium and osmium. Recent calculations by Gilbert et al. [1] predict a damage level of 15 dpa after one full power year for DEMO. Behavior of tungsten under neutron bombardment was already investigated, recently using tungsten self-implantation as a proxy for neutrons. Self-implantation by tungsten ions has the advantage to avoid the introduction of additional impurities, which potentially may act as additional trap sites for hydrogen. Radiation damage, either by neutrons or heavy ions, generally increases the hydrogen retention in tungsten considerably [2,5].

At the same time (n, α) reactions will produce He throughout the bulk of plasma facing materials and structural components in a future fusion device. Recent calculations [1] predict rather low He concentrations around 4 ppm after a full power year for tungsten parts of the

divertor. On the other hand a low energetic He study [2] show that even a small amount of He (5% as a D plasma impurity) can affect the retention properties strongly. It has to be mentioned though that in contrast to the He particles from the plasma, which can not penetrate deeper into the material, the neutrons are able to penetrate – and cause He production, in the bulk material. The behavior of He introduced into the bulk has for example been investigated by Ullmaier and Chernikov [6, 7] and recently by Debelle et al. [8, 9]. He was in all cases introduced at ~ MeV energies, the authors focused on the He behavior and trapping in tungsten. Ullmaier reported about He bubbles formation up to the temperatures of about 0.45 of the tungsten melting temperature. Bubble structure and size were investigated in [7]. Recent work [8] assumes He trapping in vacancy complexes which may cluster to larger structures as gas filled bubbles under thermal treatment. In this work we continued the previous studies [5] of hydrogen retention in radiation damaged tungsten and focused on the influence of bulk He introduced into the damaged zone on hydrogen retention.

## 2. Experimental

In our study we used polycrystalline hot rolled tungsten from Plansee with a purity of 97.95 at.-%. All samples were cut from one manufacturing batch [10]. 0.8 mm thick samples 12 by 15 $mm^2$ in size were polished to a mirror finish and recrystallized at 2000 K for 10 min in vacuum ($p < 10^{-6}$ Pa). He and W implantations were performed at $10^{-6}$ Pa on a water cooled substrate holder at the 3 MV tandem accelerator laboratory of IPP Garching. For homogeneous implantation the ion beams were scanned over the whole sample surface. $W^{6+}$ ions were implanted with an energy of 20 MeV to fluences of $3\times10^{16}$ $m^{-2}$ and $1.4\times10^{18}$ $m^{-2}$. For this energy the damage profile is expected to extend up to 2.3 µm according to SRIM 2008 [13] calculations as shown in Fig. 1a. The "full cascade option", a displacement energy of 90 eV as advised in [12], and theoretical tungsten density were used. As displacement per atom (dpa) the total number of vacancies counted by SRIM was assumed. With these assumptions the applied fluencies convert to 0.02 and 0.89 dpa at the damage peak. Fig. 1a shows the damage profiles for both low and high damage level W implantations and the damage profile for the highest accumulated He fluence of $1.3\times10^{20}$ He/$m^2$. According to SRIM this converts to an average He concentration of 1000 at.-ppm within the first 2.3 µm as shown in Fig. 1b. One can see that in the 0.89 dpa W damage case the damage introduced by He ion implantation is negligible while for low dpa W samples the damage created by the He implantation dominates. The damage level for the other He fluences used can be derived by

scaling the 1000 ppm curve. The isotope $^3$He was used for all implantations instead of $^4$He due to the possibility to measure it quantitatively in tungsten by nuclear reaction analysis (NRA). Eleven different energies ranging from 500 keV to 1500 keV were applied in steps of 100 keV to achieve a relatively homogenous $^3$He concentration which covers most of the W damaged zone as it is shown in Fig. 1b. Because the lowest energy possible was 500 keV, the damage as well as the He concentration is reduced in the first 500 nm. The implanted He amount was measured ex-situ using the $^3$He(d, p)$^4$He nuclear reaction at a reaction angle of 135° using a PIPS-detector with 2000 µm depletion depth, a solid angle of 29.9 msr, and stopper foils of 5 µm Ni and 12 µm Mylar. The detected proton counts were converted to $^3$He content by using the total cross section data from Möller et. al [14] assuming angular independence in the center-of-mass system. The samples were loaded with deuterium at the ECR plasma device PlaQ [10]. Five samples were exposed at the same time. The temperature of the samples was monitored by an IR camera and a thermocouple mounted on the sample holder. During loading the samples were kept at 400 K by a thermostat. No bias was applied to the sample holder resulting in a floating potential around 15 eV. The particle flux consists mainly of $D_3^+$ with small fractions of $D_2^+$ and $D^+$. The total D flux is $5\times10^{19}$ D/m$^2$. For these low ion energies no damage is expected to be introduced into the very near surface layer because it is well below the threshold value. The implantation fluence was chosen based on a previous study [5] on saturation effects in damaged tungsten. There after 20 h of implantation at the same plasma conditions almost saturated depth profiles were obtained. A 72 h implantation did not change the depth profiles much. Since we implant D at slightly lower sample temperature as in [5] we used 48 h which is a mean value between both times. During these 48 h a D fluence of ~ $10^{25}$ m$^{-2}$ is accumulated.

After the samples were loaded NRA measurements of retained D amounts were performed using the D($^3$He,p)$^4$He and D($^3$He,$^4$He)p reactions. The same detector as described above was used for detecting the protons. Seven different energies of the analysing $^3$He$^+$ ion beam were applied, ranging from 500 to 4500 keV to probe different sample depths [15]. At low energies the alphas were detected at a reaction angle of 102° with a 700 µm thick PIPS detector in order to achieve a good depth resolution in the near surface layer [17]. At energies of 1200 keV and higher only protons were detected. Finally the spectra were deconvoluted using the SIMNRA [11] and NRADC [18] codes in order to obtain D depth profiles up to the depth of 7.8 µm. Integration of these depth profiles over depth delivers the amount of D within these 7.8 µm.

The total amounts of D retained in the samples were measured by thermal desorption spectroscopy (TDS). These measurements were performed at the TESS setup (IPP, Garching)[19]. The samples were installed in a glass tube, the base pressure was in the $10^{-7}$ – $10^{-8}$ mbar range during the heating ramp. An oven which can be moved along the glass tube is used for sample heating in this setup. We used the same heating ramp of 15 K/min for all the measurements in this study. The maximum oven temperature was $T_{max}$ = 1323 K. The sample temperature was calibrated using a thermocouple spot welded directly to one sample. The gas composition during the measurement was monitored by a Pfeiffer DMM 422 quadrupole mass spectrometer in multi ion detection mode, collecting mass channels from 2 to 48 amu/q. After every TDS measurement a background run – a ramp with no sample in the heated area of the tube – was performed to control the residual background signals, most importantly those where D release might take place – $D_2$, HD, $D_2O$, HDO. After all measurements a calibration of the QMS was performed using calibrated $D_2$ and HD leaks. The signal of mass 3 (HD) was more than 2 orders of magnitude smaller compared with the mass 4 ($D_2$) signal, the signal was almost the same for measurements with sample and for background measurements. Taking this into account the contribution of the mass 3 signal to the total D desorption fluence was neglected in our case. For calculation of the desorbed D amount we took only the mass 4 signal into account. Using the calibration factors taken from the calibration leak measurements the QMS output counts were converted to a desorption flux. The total amount of retained D was calculated by integrating the $D_2$ desorption flux over the measurement time. To monitor the $^3$He desorption a high resolution mass spectrometer (MKS Instruments Micro Vision Plus) was used to measure the mass 3 signal. The mass resolution of this QMS allows to distinguish between HD and $^3$He.

After TDS NRA was performed again to check for the remaining D content. The NRA spectra contained only little intensity close to the noise level which correspond to a remaining amount of D in the range of ~ 1 % of the initial D amount. Within the uncertainty of the method this amount can be treated as negligible. So we assume that during TDS all D retained in the sample was desorbed.

## 3. Results and discussion

In a first step the thermal behavior of the implanted $^3$He was investigated by measuring the total amount of $^3$He before and after TDS using the $^3$He(D,p)$^4$He reaction. The amounts of $^3$He before and after TDS until 1200 K were detected to be similar within the

uncertainties of the NRA measurements, for example $1.53\times10^{20}$ $m^{-2}$ before and $1.62\times10^{20}$ $m^{-2}$ after the TDS for the 1000 ppm specimen. This means, that the implanted $^3$He is not released until 1200 K. This is confirmed by the measured TDS spectra, where no significant additional release of mass 3 above the HD level was observed: For the 1000 ppm specimen the release of $^3$He was below about 2 % of the total implanted amount. For our implantation energy range it was reported by other authors before that up to 2000 K no He desorption was observed [8]. Chernikov and Trinkaus published in [7] that heating of tungsten samples implanted with He results in a formation of nano-sized bubbles, containing He at a rather high pressure. The size of these bubbles depends on the heating temperature. For the maximum temperature of 1200 K in our case bubbles of ~ 1 nm in size are expected. After TDS and following NRA measurement the samples were heated in vacuum up to 2000 K, after this heating procedure the NRA measurement of the $^3$He amount was repeated. It showed again no significant difference in $^3$He concentration before and after heating within the uncertainty of the measurement. So from our data we can say, that up to 2000 K no He desorption takes place. These results are in contrast to low-energetic implantation of He into W, where release of He is observed already at temperatures below 1000 K [2, 4].

To investigate the influence of He on D retention in radiation-damaged W we first prepared a series of five samples – a reference without $^3$He, and four samples with $^3$He fluences ranging from $1\times10^{18}$ to $1\times10^{20}$ $m^{-2}$ which converts to mean concentrations ranging from 10 ppm to 1000 ppm. The additional damage created by the $^3$He ions implantation is below 0.05 dpa in the damage peak for the highest $^3$He fluence, and accordingly lower for the smaller fluences. All samples were pre-damaged by W ions to a damage level of 0.89 dpa in the damage peak before $^3$He implantation. Effects of damage on deuterium retention saturate in the range 0.5-1 dpa [5]. We therefore expect that the influence of the additional damage by the $^3$He is negligible. Therefore the difference in D retention which may appear can be ascribed to the presence of $^3$He atoms rather than He damage.

The D depth profiles of all samples are rather similar. All profiles show a surface coverage of about $2\times10^{19}$ $D/m^2$, which cannot be resolved within our depth resolution of about 20 nm. We attribute this to either adsorption at the surface or implantation within the ion range. However, this surface coverage has only a very small contribution to the total amount of retained D. This surface peak is followed by a plateau extending up to a depth of 2.3 μm, i.e. up to the end of the damaged zone. This plateau ends in a sharp concentration drop. Within the uncertainty of the measurement there is no significant difference observed, neither in the range nor in the height of the plateau between the samples containing $^3$He and

the reference sample without $^3$He. Thus we observed no significant change in D retention within the damaged zone in the presence of $^3$He. The retention is still governed by the traps; the high concentration of those is due to the W ion implantation. Behind the damaged zone at the depths larger than 2.3 μm a difference between the depth profiles of the samples containing $^3$He and the reference sample exists. In Fig. 2 the D depth profiles of the $^3$He implanted samples and the reference sample are plotted together with the W damage profile. Behind the damaged zone the concentration for the reference sample is around 0.01 at. %, the 100 ppm sample lies slightly above this level, while the high fluence He implanted samples show one order of magnitude higher D concentration between the 2.3 and 7.8 μm depth. In Fig. 3 the total D amount is shown as a function of the implanted He amount. The open blue data points show the amount obtained by integration of the depth profiles measured by NRA. These values correspond to the amount of D retained within the first 7.8 μm of the sample. The integrated NRA data show a small rise of around 20 % between the reference and the highest He fluence samples. From the depth profile data (see Fig. 2) this increase is attributed to the D retention behind the plateau between 2.3 und 7.8 μm. Since the material has not been directly modified there (maximum range of both W and $^3$He implantations is ~ 2.3 μm according to SRIM calculations) we can only assume at this point that implantation of ~ $10^{20}$ He/m$^2$ (500 and 1000 ppm samples) results in the formation of stress fields which in contrast to the He atoms themselves and radiation damage caused by implantation extend up to depths beyond the implantation range. In addition, Fig. 3 shows the results of the TDS measurements (filled red data points). They correspond to the total amount of D retained within the whole sample. In contrast to the NRA result, TDS data points lie all on the same level of ~ $2.5\times10^{21}$ m$^{-2}$. Obviously the presence of He modifies D retention locally only within the NRA detection depth but not much beyond. Nevertheless, at these high damage levels D retention is strongly dominated by the traps introduced in the material by W ion implantation [5], so the additional effect of He is rather small in this case.

The second series was conducted at much lower W fluence in order to avoid that D retention is dominated by the traps introduced by W ion implantation. A peak damage level of 0.02 dpa was chosen. He fluence range was kept the same. For the highest He fluence, the additional damage created by He is significant and the total dpa level rises to 0.07 dpa. For the lower $^3$He fluences the additional damage is correspondingly lower,. The specimens were loaded at the same conditions as the previous series – 400 K, $1\times10^{25}$ D/m$^2$. In Fig. 4 the D depth profile and the damage profile of the sample without $^3$He are plotted as reference. For this reference sample the D depth profile extends until the end of the damaged zone, i.e. from

the surface up to a depth of about 2.3 μm. The maximum D concentration is considerably lower than in the 0.89 dpa case due to the lower damage. Furthermore the D profile for the sample implanted additionally with 1000 ppm $^3$He is plotted together with the corresponding $^3$He damage profile. In contrast to the previous series with much higher trap concentration (due to the higher W damage level) the deuterium depth profile looks different: Here the concentration drop appears already at 1.5 μm depth. The saturation of the damaged zone was obviously not achieved after 48 h. Therefore, the samples were loaded to higher fluences. It required three times higher D fluences to finally obtain saturation. In Fig. 5 the D retained within the first 7.8 μm for the reference sample and for samples implanted with three different $^3$He fluences are plotted as a function of D fluence. For the reference sample without He there is no dependence on implanted D fluence in this fluence range – implantation twice as long as the first time results in the same amount of D retained which is in line with the previous work [5] – after the first D implantation the saturation was achieved. The situation is different for the He implanted samples – there is a clear rise in retained D amount with increasing D fluence. The evolution of the depth profiles let one consider that after implantation of $3*10^{25}$ D/m$^2$ the saturation of the damaged zone was achieved and we therefore compare the D concentrations for these saturated depth profiles. From a recent study that investigated D retention as a function of W damage one would expect an increase of about a factor of three for the 1000 ppm $^3$He sample if the damage alone would be responsible for the D uptake [5]. Because we find an increase in D retention from ~ 4 to ~ $12\times10^{20}$ D/m$^2$ we can conclude that the presence of He does not affect the amount of retained D. Nevertheless, the effective diffusion coefficient is clearly affected. The reason for the slower uptake remains unclear. We can exclude that the increased number of trap sites are responsible because it is still smaller than in the first experimental series were filling was faster. To illustrate this the retained D amount of a reference sample (0.89 dpa, no He) is also shown in Fig. 5.

After the last D implantation TDS measurements of all five samples were performed. They show a larger amount of D compared to integrated NRA depth profiles, which indicates that diffusion into the bulk behind the damaged zone takes place.

**Summary**

We investigated the influence of MeV helium implantation on deuterium retention in self-damaged tungsten. $^{3}$He was implanted such that a homogeneous $^{3}$He concentration profile in the damaged zone was created. Two situations were examined – high W-damage level plus He implantation for several He fluences and low W-damage level plus He at the same He fluences as in the previous case. At high damage levels the radiation-induced damage introduced into the material by tungsten self-implantation dominates hydrogen retention. We observed no change of the maximum D concentration in the damaged zone in the presence of $^{3}$He up to concentrations of about 1000 ppm. But above 500 ppm D retention starts to increase behind the damaged zone. It results in a 20 % increase of the D amount within the first 7.8 μm for the 1000 ppm sample. Moreover the total D retention stays unaffected by the addition of $^{3}$He amounts up to ~ 1000 ppm.

In the lower W-damage level case an increase of retained D with increasing damage level was observed. It showed the same increase as it was previously reported in [2] for self-damaged tungsten without He. Even at low He concentrations of about 100 ppm the saturation of the damaged and He implanted zone with D proceeds slower compared to the reference sample without He. It required a three times higher D fluence to obtain a saturated D depth profile of He implanted samples, as compared to the reference sample.

**Acknowledgements**

The authors would like to thank T. Dürbeck for his assistance with the TDS measurements and J. Dorner and M. Fußeder for their assistance with ion implantations and ion beam analysis.

This work was supported by the Impuls- und Vernetzungsfonds of the Helmholtz Society.

**References**


1. M.R. Gilbert, S.L Dudarev, D. Nguyen-Manh, S. Zheng, L.W. Packer, J.-Ch. Sublet, J. Nucl. Mater. (2013), http://dx.doi.org/1 0.1016/j.j nucmat.2 013.03.085
2. V Kh Alimov, W M Shu, J Roth, K Sugiyama, S Lindig, M Balden, K Isobe and T Yamanishi 2009 Phys. Scr. (2009) 014048
3. Y. Ueda, H. Kashiwagi, M. Fukumoto, Y. Ohtsuka, N. Yoshida, FUSION SCIENCE AND TECHNOLOGY 56 (2009) 85
4. H.T. Lee, A.A. Haasz, J.W. Davis, R.G. Macaulay-Newcombe, D.G. Whyte, G.M. Wright Journal of Nuclear Materials 363–365 (2007) 898–903
5. T. Schwarz-Selinger, this conference
6. H. Ullmaier, Journal of Nuclear Materials 133&134 (1985) 100 104
7. V.N. Chernikov, Ju.V. Lakhotkin, H. Ullmaier, H. Trinkaus, P. Jung, H.J. Bierfeld, Journal of Nuclear Materials 212-215 (1994) 375-381
8. A. Debelle, M.F. Barthe, T. Sauvage, R. Belamhawal, A. Chelgoum, P. Desgardin, H. Labrim, Journal of Nuclear Materials 362 (2007) 181–188
9. P.E. Lhuillier, A. Debelle, T. Belhabib, A.L. Thomann, P. Desgardin, T. Sauvage, M.F. Barthe, P. Brault, Y. Tessier, Journal of Nuclear Materials, 417 (2011) 504-507
10. A. Manhard (2012), IPP Report 17/34, Max-Planck-

Institut für Plasmaphysik, Garching, Germany, original publication

11. M. Mayer (1997) SIMNRA User's Guide, IPP Report 9/113, Max-Planck-

Institut für Plasmaphysik, Garching, Germany, original publication

12. ASTM Int'l E521-96 Standard Practice for Neutron Radiation Damage Simulation by Charge Particle Irradiation, Annual Book of ASTM Standards vol 12.02 (Philadelphia, PA: American Society for Testing and Materials) p 7
13. http://srim.org
14. W. Möller, F. Besenbacher, Nuclear Instruments and Methods, 168 (1980) 111-114
15. M. Mayer, E. Gauthier, K. Sugiyama, U. von Toussaint, Nuclear Instruments and Methods in Physics Research B, 267 (2009) 506-512
16. P. Wang, W. Jacob, L. Gao, T. Dürbeck, T. Schwarz-Selinger, Nuclear Instruments and Methods in Physics Research B, 300 (2013) 54-61
17. R.A Langley, S.T Picraux, F.L Vook, Journal of Nuclear Materials 53 (1974) 257-261

18. K. Schmid, U. von Toussaint, Nuclear Instruments and Methods in Physics Research B, 281 (2012) 64
19. E. Salançon, T. Dürbeck, T. Schwarz-Selinger, F. Genoese, W. Jacob, Journal of Nuclear Materials, 376 (2008) 160-168
20. R. Jarjis, Nuclear Cross-section Data for Surface Analysis, vol. 1. University of Manchester, England, 1979

**Figure captions:**

Fig. 1: Damage (1a) and implantation (1b) profiles for the highest He fluence (1000 ppm). The damage profiles for both high and low W fluence ion implantation are plotted in 1a as dashed lines for comparison.

Fig. 2: D depth profiles after plasma loading at floating potential for the high W damage level series for different $^{3}$He concentrations.

Fig. 3: Comparison of total retained D amounts taken from NRA and TDS as a function of He fluence for high W damage level series.

Fig. 4: Evolution of D depth profile during loadings for the 1000 ppm He implanted sample for low W damage level series.

Fig. 5: Total retained D amounts taken from NRA and TDS as a function of D fluence for low W damage level series. The lines are plotted to guide the eye. The 0.89 dpa data point is plotted for comparison

**Figures**

Fig. 1

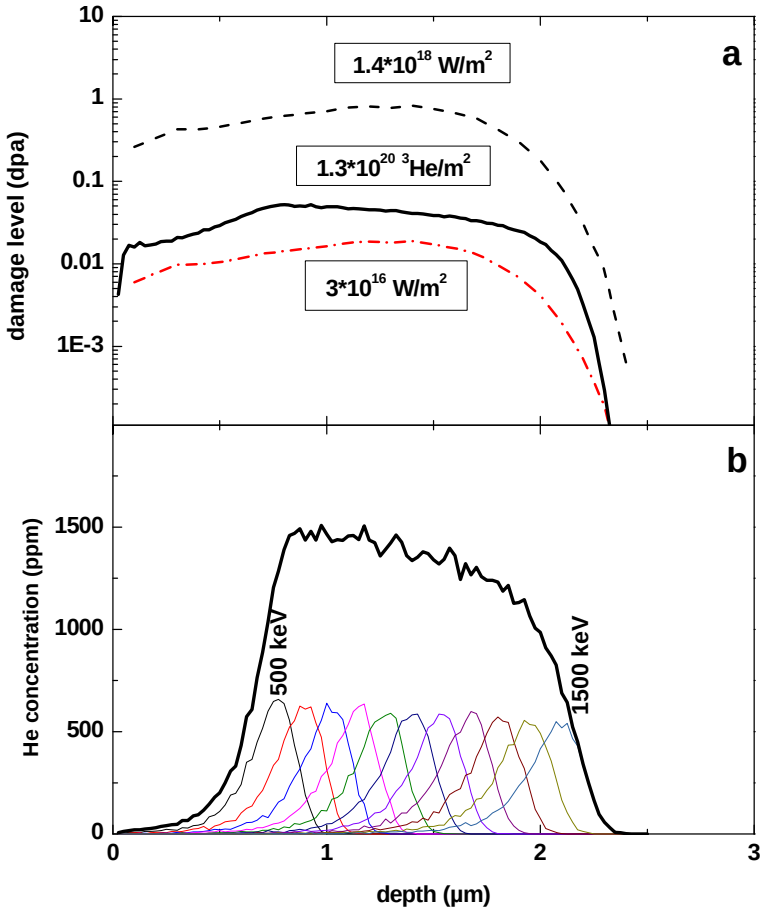

Fig. 2

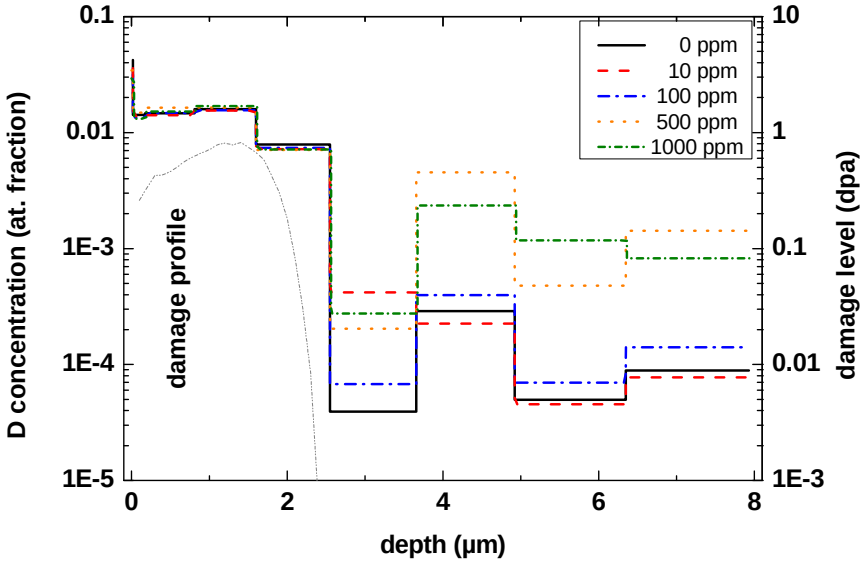
0.1
0.01
1E-3
1E-4
1E-5
D concentration (at. fraction)
damage profile
0
2
4
6
8
depth (μm)
10
1
0.1
0.01
1E-3
damage level (dpa)
0 ppm
10 ppm
100 ppm
500 ppm
1000 ppm

Fig. 3

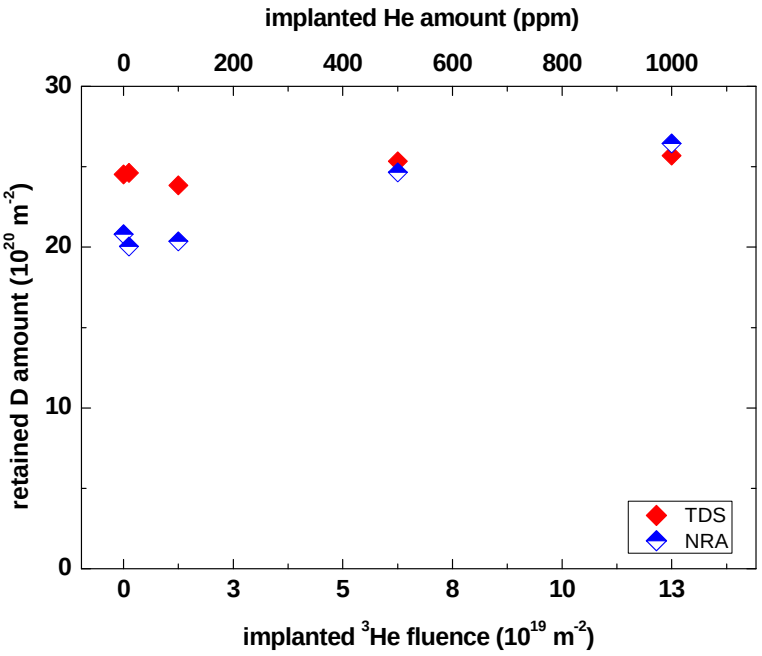
implanted He amount (ppm)
0
200
400
600
800
1000
30
20
10
0
retained D amount ($10^{20}$ $m^{-2}$)
TDS
NRA
0
3
5
8
10
13
implanted $^{3}$He fluence ($10^{19}$ $m^{-2}$)

Fig. 4

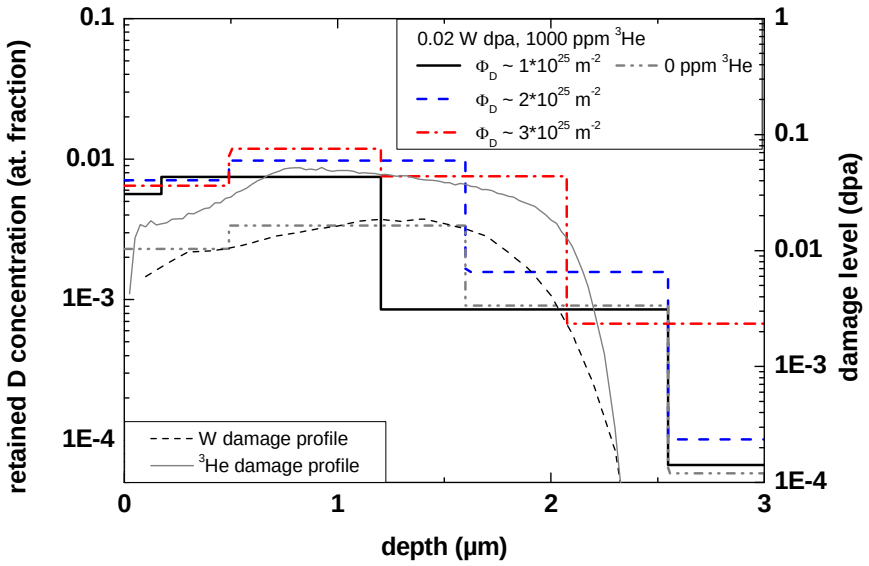
0.02 W dpa, 1000 ppm 3He
ΦD ~ 1*10^25 m^-2
0 ppm 3He
ΦD ~ 2*10^25 m^-2
ΦD ~ 3*10^25 m^-2
W damage profile
3He damage profile
retained D concentration (at. fraction)
damage level (dpa)
depth (μm)
0.1
0.01
1E-3
1E-4
1
0.1
0.01
1E-3
1E-4
0
1
2
3

Fig. 5

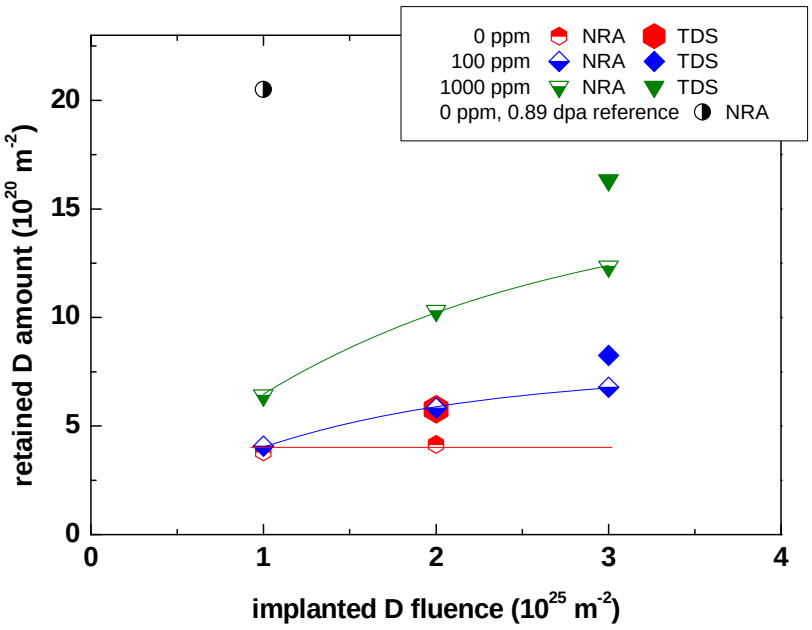
0 ppm NRA TDS
100 ppm NRA TDS
1000 ppm NRA TDS
0 ppm, 0.89 dpa reference NRA
retained D amount ($10^{20}$ $m^{-2}$)
implanted D fluence ($10^{25}$ $m^{-2}$)
0
5
10
15
20
0
1
2
3
4